HHS Public Access

Author manuscript

Cell Rep. Author manuscript; available in PMC 2019 January 08.

Published in final edited form as:

Cell Rep. 2018 December 04; 25(10): 2797–2807.e8. doi:10.1016/j.celrep.2018.11.024.

The HDAC-Associated Sin3B Protein Represses DREAM Complex Targets and Cooperates with APC/C to Promote Quiescence

Anthony J. Bainor[1], **Siddharth Saini**[2], **Alexander Calderon**[1], **Raquel Casado-Polanco**[1], **Belén Giner-Ramirez**[1], **Claudia Moncada**[1], **David J. Cantor**[1], **Amanda Ernlund**[3], **Larisa Litovchick**[2], and **Gregory David**[1,4,5,6,*]

[1]Department of Biochemistry and Molecular Pharmacology, NYU Langone Medical Center, New York, NY 10016, USA

[2]Department of Internal Medicine and Massey Cancer Center, Virginia Commonwealth University, Richmond, VA 23298, USA

[3]Department of Microbiology, NYU Langone Medical Center, New York, NY 10016, USA

[4]Department of Urology, NYU Langone Medical Center, New York, NY 10016, USA

[5]NYU Cancer Institute, NYU Langone Medical Center, New York, NY 10016, USA

[6]Lead Contact

SUMMARY

The mammalian DREAM complex is responsible for the transcriptional repression of hundreds of cell-cycle-related genes in quiescence. How the DREAM complex recruits chromatin-modifying entities to aid in its repression remains unknown. Using unbiased proteomics analysis, we have uncovered a robust association between the chromatin-associated Sin3B protein and the DREAM complex. We have determined that genetic inactivation of Sin3B results in the de-repression of DREAM target genes during quiescence but is insufficient to allow quiescent cells to resume proliferation. However, inactivation of APC/C^{CDH1} was sufficient for $Sin3B^{-/-}$ cells, but not parental cells, to re-enter the cell cycle. These studies identify Sin3B as a transcriptional corepressor associated with the DREAM complex in quiescence and reveals a functional cooperation between E2F target repression and APC/C^{CDH1} in the negative regulation of cell-cycle progression.

*Correspondence: gregory.david@nyumc.org.

AUTHOR CONTRIBUTIONS

Conceptualization, A.J.B., L.L., and G.D.; Methodology, A.J.B., S.S., A.C., L.L., and G.D; Investigation, A.J.B., S.S., A.C., R.C.-P., B.G.-R., C.M., D.J.C., and G.D.; Writing – Original Draft, A.J.B., A.C., and G.D.; Writing – Review & Editing, A.J.B., L.L., and G.D.; Formal Analysis, A.J.B., S.S., A.C., A.E., L.L., and G.D.; Funding Acquisition, L.L. and G.D.; Supervision, L.L. and G.D.

SUPPLEMENTAL INFORMATION

Supplemental Information includes five figures and can be found with this article online at https://doi.org/10.1016/j.celrep.2018.11.024.

DECLARATION OF INTERESTS

The authors declare no competing interests.

Graphical abstract

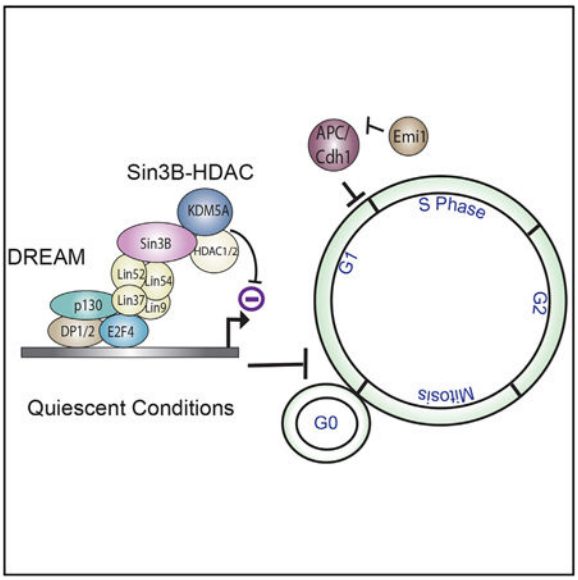

In Brief

The DREAM complex associates with the co-repressor Sin3B to repress target genes during quiescence. Bainor et al. show that Sin3B inactivation is insufficient to allow S-phase re-entry but poises quiescent cells to proliferate upon inhibition of the APC/C^{CDH1} complex, highlighting a functional cooperation between transcriptional and post-translational cell-cycle regulation.

INTRODUCTION

The progression through the cell cycle is exquisitely regulated at multiple levels. Genes are actively transcribed and repressed, and proteins are modified and/or degraded in a series of highly ordered processes. At the transcriptional level, E2F transcription factors represent critical regulators of cell-cycle progression. These proteins are clustered into transcriptional activators (E2F1, E2F2, and E2F3a) or repressors (E2F3b, E2F4–8) and are responsible for the regulation of the expression of hundreds of cell-cycle-related genes (Dimova and Dyson, 2005). E2F transcription factors are regulated primarily by the pocket protein family, which includes RB1 and the related p107 and p130 proteins. During the G_1 phase of the cell cycle, RB1 interacts with activating E2Fs and inhibits their ability to activate transcription. Additionally, p107 and p130 interact with E2F repressors to actively suppress transcription of cell-cycle genes in quiescence and early phases of the cell cycle (Beijersbergen et al., 1994; Dyson et al., 1993; Ginsberg et al., 1994; Lees et al., 1993; Vairo et al., 1995). The molecular bases underlying the ability of p107/p130 to modulate E2F target gene expression was recently elucidated in part with the identification of the highly conserved DREAM (DP, RB-like, E2F, and MuvB) complex (Litovchick et al., 2007; Osterloh et al., 2007; Pilkinton et al., 2007).

The mammalian DREAM complex is composed of p130 or p107, DP1 or DP2, and E2F4 or E2F5, and the MuvB core including LIN9, LIN37, LIN52, LIN54, and RBBP4 or RBBP7

(Sadasivam and DeCaprio, 2013). The DREAM complex localizes to the promoters of hundreds of cell-cycle-regulated genes and contributes to their repression during quiescence (Litovchick et al., 2007). Depletion studies of various members of the DREAM complex have been confounding. While the knockdown of individual subunits of DREAM leads to a transcriptional derepression of its targets, the resulting upregulations are only modest (Litovchick et al., 2007). In addition, this de-repression event is not sufficient to cause cell-cycle re-entry (Litovchick et al., 2007). However, the mutation of S28 on the MuvB subunit LIN52, a crucial phosphorylation site for the assembly of the DREAM complex, rendered cells refractory to oncogenic Rasinduced senescence (Litovchick et al., 2011). These findings are in agreement with previously shown functional compensation by all three pocket proteins for cell-cycle exit (Dannenberg et al., 2000; Sage et al., 2003). Intriguingly, there was no evidence of any chromatin-modifying proteins in the initial mass-spectrometry studies identifying the proteins associated with DREAM (Litovchick et al., 2007). A recent study, however, indicated that genetic inactivation of the DREAM component Lin37 leads to a potent de-repression of cell-cycle gene transcription in G_0/G_1 (Mages et al., 2017). As Lin37 itself does not harbor enzymatic activity, it likely recruits transcriptional co-repressors that remain to be identified.

Among the better-studied transcriptional co-repressor complexes, the Sin3/HDAC complex is characterized by the presence of the highly conserved and ubiquitously expressed Sin3 protein. Containing no DNA binding domain or enzymatic activity of its own, Sin3 has been established as a flexible scaffold protein able to assemble large, modular, repressive complex(es) (Silverstein and Ekwall, 2004). Sin3 owes its repressive activity at least in part to its direct interaction with HDAC1 and HDAC2, and in some instances, with KDM5A, and is recruited to target loci through its association with sequence-specific transcription factors (Bartke et al., 2010; Hassig et al., 1997; Hayakawa et al., 2007; Heinzel et al., 1997; Jelinic et al., 2011; Malovannaya et al., 2011; van Oevelen et al., 2008, 2010; Zhang et al., 1997). In mammals, the Sin3 family consists of two proteins, Sin3A and Sin3B, with both redundant and non-redundant functions. While *Sin3a*-deleted murine cells exhibit severe proliferation defects and massive apoptosis, *Sin3b*-deleted primary fibroblasts proliferate normally (Dannenberg et al., 2005; David et al., 2008). Interestingly, *Sin3b*-deleted cells are refractory to oncogene-induced senescence and, in some settings, exhibit altered terminal differentiation (Cantor and David, 2017; Dannenberg et al., 2005; David et al., 2008; Grandinetti et al., 2009; Riel-land et al., 2014). In addition, it has been shown that p107 and p130 specifically recruit the Sin3B/HDAC complex to promote chromatin compaction and subsequent transcriptional repression (Balciunaite et al., 2005; David et al., 2008; Rayman et al., 2002).

Here, we report that the Sin3B/HDAC complex robustly interacts with the DREAM complex in a cell-cycle-dependent manner. We demonstrate that Sin3B specifically associates with the DREAM complex during quiescence and early G_1, and retains its ability to interact with the MuvB core throughout the cell cycle. Analysis of the transcriptome revealed that deletion of Sin3B resulted in a global de-repression of established DREAM target genes. These target loci encode for cell-cycle-related proteins and are bound by Sin3B at their promoter regions. Human cancer cells lacking Sin3B were, however, able to enter quiescence normally and progress through the cell cycle with normal kinetics. Strikingly,

ectopic expression of the APC/C^{CDH1} inhibitor EMI1 was sufficient to promote cell-cycle re-entry of Sin3B deleted cells under serum-deprived conditions, while the Sin3B wild-type cells remained quiescent. This study sheds light on the ability of DREAM to recruit the chromatin-modifying Sin3B/HDAC complex to repress its target genes. This also points to the functional cooperation between APC/C^{CDH1} and DREAM in the regulation of G_1- to S-phase cell-cycle progression.

RESULTS

Sin3B Interacts with the DREAM and the MMB Complexes

To investigate the molecular mechanisms underlying Sin3B's impact on cellular proliferation, stable cell lines were generated to express FLAG-tagged Sin3B in the absence of the corresponding endogenous protein. Specifically, immortalized Sin3B-null mouse embryonic fibroblasts were infected with either a retrovirus encoding C-terminal FLAG-tagged Sin3B or with the corresponding empty retrovirus. Sin3B-associated polypeptides were affinity purified using an anti-FLAG antibody and identified by tandem mass spectrometry. Consistent with previous reports, we identified several members of the canonical Sin3-HDAC complex, which include the following: Sin3A, HDAC1, HDAC2, RBBP7, SAP130, ARID4B, ING1, ING2, SUDS3, SAP30, SAP30L, BRMS1L, and BRMS1 (Bansal et al., 2016) (Figure 1A). Additionally, several members of a recently characterized smaller Sin3B complex were identified as well (Graveline et al., 2017; Jelinic et al., 2011). These proteins include the following: PHF12, KDM5A, EMSY, and MORF4L1. Strikingly, Sin3B immunoprecipitates contained detectable peptides corresponding to all members of the mammalian DREAM complex (DP1, p130, p107, E2F4, RBBP4, LIN9, LIN37, and LIN54), except for LIN52 (Figure 1A). The interaction between Sin3B and the DREAM component LIN9 was confirmed by immunoprecipitation in T98G cells, following transient co-expression of the two proteins (Figure 1B). Additionally, ectopically expressed Sin3B was able to associated with endogenous DREAM components LIN9, LIN37, p107, and p130 (Figure 1C). The MuvB complex dissociates from DP1-p130-E2F4 as cells progress through the cell cycle, to form a stable complex with BMYB in G_1/S called MMB, and then an independent complex with FOXM1 in S phase (Sadasivam et al., 2012). Interestingly, BMYB was detected as a Sin3B-associated protein (Figure 1A), and the corresponding interaction was confirmed by co-immunoprecipitation (co-IP) in Sin3B-transfected T98G cells (Figure 1C). In contrast, we were unable to detect FOXM1 in the $Sin3B^{FLAG}$ immunoprecipitates by mass spectrometry, or detect an interaction between Sin3B and FOXM1 upon co-expression in 293T cells, while we successfully detected components of the DREAM and MMB complexes in this assay (Figure S1). Taken together, these results indicate that Sin3B interacts with the DREAM complex, as well as with the MMB complex, but likely not with the MuvB-FOXM1 complex.

The Sin3B/DREAM Interaction Is Established in Quiescent Cells

The human DREAM complex has been previously characterized using the human glioblastoma cell line T98G (Litovchick et al., 2007). To further validate our findings, we demonstrated that endogenous LIN37, an integral member of the MuvB complex, associates with both endogenous and exogenous Sin3B in asynchronous human T98G cells (Figure

2A). We also confirmed this interaction using mouse NIH 3T3 cells (Figure 2A). Finally, immunoprecipitation with an anti-Sin3B antibody revealed an association with additional members of the DREAM complex, namely LIN9, LIN37, and p130 at the endogenous level, thus confirming a specific and robust interaction between Sin3B and the DREAM complex (Figure 2B).

As mentioned above, the mammalian DREAM complex is present in G_0/G_1 but dissociates in late G_1, releasing the MuvB core from p130 and E2F4. Since we performed our initial analysis in asynchronously cycling cells, we tested the interaction of Sin3B with DREAM complex components in synchronized cells. T98G cells were rendered quiescent by serum deprivation for 72 hr, prior to immunoprecipitation. As expected, Sin3B robustly associated with the MuvB components LIN9 and LIN37 in both the cycling and serum-starved cells, whereas the DREAM-specific p130 interacted more strongly in quiescent cells (Figure 2B). To investigate the interaction between Sin3B and the DREAM complex components as cells progress through the cell cycle, quiescent T98G cells were released into serum-containing medium, and Sin3B immunoprecipitations were performed at various time points. As shown in Figure 2C, Sin3B associates with p130 in G_0 and G_1, but not at later cell-cycle phases, consistent with the well-established dissociation of p130 from MuvB past the mid-G_1 point caused by increased activity of CDK4/6 and CDK2 (Guiley et al., 2015; Litovchick et al., 2007; Odajima et al., 2016; Tedesco et al., 2002). Strikingly, the interaction between Sin3B and the MuvB core components LIN9 and LIN37 is retained throughout G_1 and S phases. Consistent with the upregulation of LIN9 during cell-cycle progression, the association between Sin3B and LIN9 increases as cells progressed through the cell cycle (Figure 2C). Since MuvB interacts with p130 and BMYB in different phases of the cell cycle, our results suggest that Sin3B interacts with the MuvB core components independently of p130 or BMYB. To confirm the hypothesis that Sin3B interacts with the MuvB core components independently of the Rb-related pocket proteins, we tested the ability of Sin3B to associate with LIN9 and LIN37 in immortalized mouse embryonic fibroblasts (MEFs) genetically inactivated for Rb, p107, and p130 (TKO [triple knockout] [Dannenberg et al., 2000]). As shown in Figure 2D, the interaction between Sin3B and MuvB core components was not affected by the absence of Rb-related pocket proteins.

DREAM Interacts with Sin3B through the PAH3/HID

Sin3B contains several well-characterized domains responsible for its interaction with different partners such as HDAC1 (Silverstein and Ekwall, 2004). To identify Sin3B domains responsible for its interaction with MuvB, we generated truncation mutants of Sin3B (Figure S2A). We then performed immunoprecipitations using these mutants and probed for the association with LIN9. As shown in Figure S2B, mutants containing the PAH1 and PAH2 domains, or the HCR domain only, were unable to interact with LIN9. However, all Sin3B mutants containing the PAH3/HID domains were able to associate with LIN9. Taken together, these results suggest that DREAM interacts with Sin3B through the PAH3/HID, independently of the Sin3B-HDAC1 interaction.

Sin3B Is Required for the Transcriptional Repression of DREAM Target Genes

Previous studies have demonstrated that an integral DREAM complex is required for the repression of more than 800 cell-cycle-related genes (Sadasivam and DeCaprio, 2013). Based on the robust interaction detected between Sin3B and the DREAM complex, and the lack of repressive activity within the known components of the DREAM complex, we hypothesized that Sin3B tethers the enzymatic activities required for DREAM targets' repression. To test this, Sin3B was genetically deleted in T98G cells via CRISPR/Cas9, resulting in the isolation of knockout clones from two independent Sin3B-targeting sgRNA pairs, and wild-type clones using the same guide pairs (Figure 3A). Sin3B-deleted T98G cells were then synchronized by serum starvation and released into serum-containing medium. Protein expression levels of specific DREAM targets were evaluated at different stages of the cell cycle. Notably, Sin3B inactivation resulted in the premature upregulation of cyclin A2 (encoded by the DREAM target gene *CCNA2*) in Sin3B-deleted cells in G_0, compared to their wild-type counterparts (Figure 3A). Importantly, we confirmed these results using a short hairpin RNA (shRNA) construct to knock down Sin3B expression (Figure S3). Indeed, cyclin A2 and cyclin F were found upregulated in quiescent Sin3B-depleted cells, and their levels continued to increase as the cells progressed through the cell cycle after released into serum-containing medium, indicating that Sin3B likely restricts the expression of these proteins at least during early phases of the cell cycle.

To gain insight into the repressive function of Sin3B on a genome-wide scale, the Sin3B-dependent transcriptome was investigated by RNA sequencing using two wild-type and two Sin3B-deleted T98G cell lines at different time points after release in serum-containing medium corresponding to G_0, G_1, and G_1/S phases (Figure 3B). Differential expression analysis identified 429 genes de-repressed specifically in Sin3B-deleted cells in G_0. Interestingly, fewer transcripts exhibited Sin3B-dependent de-repression in G_1 or S phase, compared to the number of genes repressed by Sin3B in G_0 (Figure 3B). Gene ontology (GO) analysis and gene set enrichment analysis (GSEA) of the genes significantly altered upon Sin3B inactivation in G_0 reveal a significant enrichment in cell-cycle- and DNA synthesis-related processes (Figure S4) Chen et al., 2013; Kuleshov et al., 2016). Using the DREAM target network database (Fischer et al., 2016), we determined that, out of the 429 genes specifically de-repressed in the absence of Sin3B in G_0, 140 genes (33%) were previously established as DREAM targets. Chromatin immunoprecipitation enrichment analysis (ChEA) and transcription factor binding analyses on these genes indicate a significant enrichment for E2F4/7, E2F1, and Sin3A potential binding sites in the promoter regions of these loci (Chen et al., 2013; Kuleshov et al., 2016) (Figure S4). Notably, Sin3B directly binds 108 (77%) of these 140 DREAM targets in other cellular systems (van Oevelen et al., 2010). We confirmed the Sin3B deletion-induced derepression of several E2F/DREAM targets using qRT-PCR in independent Sin3B-null cell lines (Figure 3C). Importantly, ectopic expression of Sin3B was sufficient to rescue the transcriptional repression of these DREAM targets in Sin3B-null quiescent cells (Figure 3D). Finally, we verified the enrichment of Sin3B on several DREAM target promoters regions in quiescent cells using chromatin immunoprecipitation (ChIP) (Figure 3E). In these experiments, genetic inactivation of Sin3B did not significantly alter the recruitment of the DREAM complex to these DNA regions, as evidenced by similar E2F4 ChIP-qPCR signals in

quiescent Sin3B-null and control cells (Figure 3E). However, histone acetylation was significantly increased at DREAM target loci upon loss of Sin3B, consistent with the model that Sin3B tethers HDAC activity to the DREAM targets in quiescence. Of note, a potent HDAC activity was found associated with Sin3B throughout cell-cycle progression (data not shown), suggesting that the repressive activity of the complex is dictated by its recruitment to target loci rather than the modulation of its activity throughout cell-cycle progression. Taken together, these results strongly suggest that Sin3B mediates the repressive function of DREAM in order to silence the expression of cell-cycle-regulated genes in quiescence, through its ability to tether histone modifiers to chromatin.

Sin3B Is Dispensable for Entry into Quiescence in Human Cells

Having established a role for Sin3B in the transcriptional repression of DREAM target genes in quiescence, we investigated the functional relevance of this observation on cell-cycle progression. To induce quiescence, Sin3B-deleted T98G cells and the parental cells were serum-starved for 72 hr (Figure 4A). At this time point, no apparent difference in KI67 positivity was observed between Sin3B wild-type and Sin3B-null cells (Figures 4B and 4C). Consistently, bromodeoxyuridine (BrdU) incorporation, indicative of replication, was only marginally increased in Sin3B-null quiescent cells versus Sin3B wild-type quiescent cells, but these differences failed to reach significance (Figures 4D–4F). Taken together, these results indicate that loss of Sin3B alone appears to be insufficient to disrupt entry into quiescence in human cells.

We also documented the effect of Sin3B deletion on the kinetics of cell-cycle re-entry. Serum-starved Sin3B-deleted cells were released into serum-containing medium, and cells were collected and analyzed at T0 (G_0), T10 (G_1), and T18 (G_1/S). Propidium iodide staining failed to reveal any significant differences in DNA content between Sin3B wild-type and Sin3B-null cells at any of these time points (Figure 4G). We further validated this finding using the FUCCI cell-cycle probes system (Sakaue-Sawano et al., 2008), whereby we determined that cells lacking Sin3B progress through the cell cycle following release into serum-containing medium at the rates comparable to that of Sin3B wild-type cells (Figure 4H). These data suggest that Sin3B is dispensable for entry into quiescence and subsequent re-entry into the cell cycle, consistent with previously reported phenotypes of cells depleted of different components of the DREAM complex (Forristal et al., 2014; Mages et al., 2017).

Loss of Sin3B Primes Cells for Entry into the Cell Cycle

While the genetic inactivation of Sin3B results in the de-repression of cell-cycle-related DREAM targets during quiescence, it bears no effect on the ability of cells to enter into quiescence under serum-deprived conditions. Therefore, we hypothesized that, in the absence of mitogenic signals, Sin3B-deleted cells do not progress to S phase because of their inability to bypass the G_1/S restriction point. To test this, we inhibited APC/C^{CDH1}, an E3 ubiquitin ligase that contributes to the maintenance of quiescence by promoting the degradation of positive cell-cycle regulators such as cyclin A2. To this end, EMI1, a negative regulator of APC/C^{CDH1} (Reimann et al., 2001), was ectopically expressed under control of tet-inducible promoter in either wild-type or Sin3B-null cells expressing the FUCCI cell-cycle probes (Figure 5A). Serum-starved cells were treated with doxycycline to induce

EMI1 expression, and cell-cycle progression was assessed via FUCCI probe positivity over 48 hr. Cells were kept in serum-free medium throughout the experiment. Intriguingly, cyclin A2 levels remained low in the wild-type cells regardless of EMI1 levels but increased noticeably in Sin3B knockout cells following doxycycline administration, correlating with the increased expression of EMI1 (Figure 5A). Parental cells exhibited marginal GFP positivity prior to EMI1 induction, which only slightly increased with EMI1 expression (10%, 14%, and 19% GFP positive at 0 hr [T0], 24 hr [T24], and 48 hr [T48] after doxycycline administration, respectively). Strikingly, Sin3B knockout cells exhibited a dramatic increase in GFP-positive cells following EMI1 induction (11%–15% at T0, 30%–36% at T24, and 51%–53% at T48) (Figure 5B). As increased GFP expression in this system could reflect the increased stability of the FUCCI reporter upon APC/C inactivation, independent of cell-cycle progression, we also assessed S-phase entry using BrdU incorporation. This approach confirmed that serumstarved Sin3B knockout cells expressing EMI1 entered S phase at a higher rate than their wild-type counterparts (Figure S5). Notably, a slight increase in the ability of $Sin3B^{-/-}$ cells to exit quiescent was noted prior to doxycycline administration, likely reflecting the leakiness of the inducible Emi-1 expression system. Finally, these results were corroborated by monitoring the effect of proTAME, a potent APC/C^{CDH1} inhibitor. While proTAME administration did not affect the ability of wild-type cells to remain in G_0 in serum-deprived conditions, the addition of proTAME led to a noticeable and significant entry into the cell cycle of Sin3B-deleted cells (Figure 5C). Together, these results indicate that, while insufficient to promote cell-cycle entry, genetic inactivation of Sin3B primes quiescent cells for cell-cycle progression through the de-repression of cell-cycle-related DREAM target genes.

DISCUSSION

We demonstrate here that the scaffold protein Sin3B associates with the DREAM complex, a master regulator of transcriptional control of the cell-cycle genes in quiescence. Our study further indicates that Sin3B carries the long-sought-after repressive activity associated with the DREAM complex, and its inactivation results in the hyper-acetylation of DREAM target promoter regions and transcriptional de-repression of the corresponding genes. Thus, this study establishes the functional relevance of the interaction between Sin3B and the DREAM complex in quiescence. While a prior study had suggested an interaction between DREAM and Sin3B-HDAC1, it did not test the functional relevance of this interaction (Sandoval et al., 2009). Our mass spectrometry results also demonstrate that Sin3B interacts with BMYB. The MuvB core has been shown to exhibit mutual exclusivity between its interaction with p130 and BMYB during the cell-cycle progression in mammalian cells (Litovchick et al., 2007; Pilkinton et al., 2007; Sadasivam et al., 2012; Schmit et al., 2007). Upon entry into G_1/S, p130 dissociates from the MuvB core and is replaced by BMYB to form the BMYB/MuvB (MMB) complex. This complex is recruited to a subset of E2F targets, primarily late S-phase genes, and its subsequent phosphorylation by cyclin A/CDK2 further results in the recruitment of the transcriptional activator FOXM1 (Sadasivam et al., 2012; Saville and Watson, 1998). Whether this MMB complex harbors a transcriptional repressive activity, or it merely serves as an intermediate complex between the repressive DREAM and the

activating FOXM1/MuvB, remains unclear. Our demonstration that Sin3B interacts with BMYB suggests the former possibility.

The MuvB complex was first identified in *C. elegans* (Harrison et al., 2006). Additional screens to detect genes that antagonize Ras signaling through the *SynMuv* pathway in the *C. elegans* vulva identified several components of the Sin3 complex, namely *hda1* and *lin-53* (homologs of HDAC1/2 and RbAP46/48, respectively) (Solari and Ahringer, 2000). However, multiple components of the HDAC-containing complex NuRD were also identified in this pathway (Solari and Ahringer, 2000), pointing to the involvement of this complex, rather than the *C. elegans Sin3* complex. It is, however, important to note that *C. elegans* only has one Sin3 protein, suggesting that a specific Sin3B-related complex may have appeared later in evolution.

Additionally, we have shown that the interaction between DREAM and Sin3B requires an intact PAH3/HID. This result is consistent with the previous demonstration that Sin3 proteins interact with the pocket proteins through adaptors such as ARID4B and SAP30 through PAH3 (Lai et al., 2001). Importantly, our observation that Sin3B interacts with both p130 and BMYB implies that this interaction is mediated by the MuvB core that is shared between both the DREAM and MMB complexes, consistent with the demonstration that Sin3B interacts with MuvB components independently of the Rb-related pocket proteins.

RNA sequencing analysis revealed that Sin3B represses the expression of 140 DREAM target genes in quiescence. The actual number of annotated DREAM targets ranges between approximately 400 and 800 genes (Litovchick et al., 2007), raising questions about the generality of Sin3B requirement in DREAM repression. The discrepancy between the number of genes derepressed in Sin3B knockout cells and the number of established DREAM targets may stem from the stringency level used in our statistical analysis. Indeed, various DREAM target genes that did not meet the false discovery rate (FDR) cutoff were found to be de-repressed in the two Sin3B knockout cell lines, but at variable levels. Alternatively, there may be some functional compensation by Sin3A in the absence of Sin3B. Indeed, our mass spectrometry analysis showed that Sin3A was among the top interactors of Sin3B (Figure 1A). This observation underscores the need to better define how DREAM and Sin3B are interacting, and whether Sin3A and DREAM can interact independently of Sin3B. Furthermore, identification of an adaptor protein that serves as a potential bridge between the Sin3B and DREAM complexes may further aid in the elucidation of these interactions. Indeed, a recent study showed that LIN37 is essential for the repressive activity associated with the DREAM complex (Mages et al., 2017), suggesting the possibility that LIN37 could tether Sin3B to the DREAM target promoters.

Consistent with the absence of cell-cycle re-entry observed in cells inactivated for different components of the DREAM complex, we demonstrate here that Sin3B inactivation is not sufficient to allow quiescent cells to resume proliferation. However, we have recently demonstrated that hematopoietic stem cells genetically inactivated for Sin3B exhibit a modest defect in their ability to remain quiescent (Cantor and David, 2017). These observations suggest that, under specific conditions, Sin3B inactivation allows quiescent cells to resume proliferation. A recent study revealed that simultaneous deletion of LIN37

and pRb allows quiescent cells to enter S phase (Mages et al., 2017). It is thus likely that dual inactivation of Sin3B and Rb would similarly result in the inability of cells to remain quiescent in low-serum conditions. Here, we show that Sin3B-null cells are sensitive to EMI1-induced cell-cycle re-entry, while Sin3B-expressing cells are not. Therefore, we hypothesize that an APC/C^{CDH1} -dependent G_1/S restriction point precludes cycling of quiescent Sin3B-deleted cells. Interestingly, a genetic screen in *C. elegans* identified *fzr-1*, the homolog of Cdh1, as a gene whose mutation is synthetic lethal with mutations in *lin-35*, the homolog of Rb and the related Rb proteins, pointing to a genetic interaction between APC/C^{CDH1} and the SynMuv B group of genes (Fay et al., 2002). Finally, it is notable that Sin3B inactivation prevents oncogene-induced senescence, both *in vitro* and *in vivo*. This is reminiscent of what has been reported for the DREAM complex, whereby its inactivation allows the cells to escape from Ras-induced senescence (Bainor et al., 2017; Grandinetti et al., 2009; Litovchick et al., 2011; Rielland et al., 2014; Tschöp et al., 2011). Whether activation of the DREAM-Sin3B-dependent repression of cell-cycle genes can serve as a tumor suppressor mechanism *in vivo* remains unclear. Furthermore, the identity of the additional events that sensitize Sin3B-DREAM-null cells to transformation remains to be elucidated, but this study warrants further investigation of the contribution of this transcriptional repression pathway in the biological settings of uncontrolled proliferation.

STAR ★METHODS

CONTACT FOR REAGENT AND RESOURCE SHARING

Further information and requests for resources and reagetns should be directed to and will be fullfilled by the Lead contact, Gregory David (gregory.david@nyumc.org).

EXPERIMENTAL MODEL AND SUBJECT DETAILS

Cell culture—MEFs (both males and females) were cultured in DMEM (Cellgro), 10% fetal bovine serum, 1% Penicillin/Streptomycin (Cellgro), 2.5 μg/mL Puromycin (GIBCO), and 50 μg/mL Hygromycin B (Invitrogen). T98G cells (glioblastoma cells from a male individual, obtained from ATCC) were cultured in DMEM (Cellgro), 10% fetal bovine serum, and 1% penicillin/streptomycin (Cellgro). T98G cells with RNAi were cultured in DMEM (Cellgro), 10% fetal bovine serum, 1% penicillin/streptomycin (Cellgro), and 1 μg/mL Puromycin (GIBCO). T98G cells engineered with the FUCCI probes and pTRIPZ-EMI1-FLAG were cultured in DMEM (Cellgro), 10% fetal bovine serum, 1% penicillin/streptomycin (Cellgro), 1 μg/mL Puromycin (GIBCO), 150 μg/mL Hygromycin B (Invitrogen), and 10 μg/mL Blasticidin (Invivogen). HEK293T cells (from a female fetus) cultured in DMEM (Cellgro), 10% donor calf serum, and 1% penicillin/streptomycin (Cellgro). NIH 3T3 cells were cultured in DMEM (Cellgro), 10% fetal bovine serum, 1% penicillin/streptomycin (Cellgro), and 2.5 μg/mL Puromycin (GIBCO). 0.5 μg/mL doxycycline was the working concentration for all doxycycline systems. All cultures were maintained in 5% CO_2 at 37°C. Regarding mice use for the generation of MEFs, all animal work was approved by the NYULMC Institutional Animal Care & Use committee.

METHOD DETAILS

Derivation of MEFs—MEFs deleted for Sin3B were isolated as previously described (David et al., 2008). Once established, cells were passaged until stochastic immortalization occurred. These cells were then clonally amplified, yielding a clonal, immortalized MEF cell line.

Establishment of Sin3B null CRISPR cell lines—T98G cells were transiently transfected with two independent sgRNA guide pairs cloned into the pX330 hSpCas9 plasmid, which targeted exon 2 of Sin3B. Cells were selected, clonally amplified and assessed for Sin3B deletion via two independent antibodies targeting Sin3B (Sin3B AK12 and Sin3B H4 listed below).

Plasmids—Stable cell lines in mouse cells were generated using the pCL vector for retroviruses. Stable cell lines in human cells were generated using VSV-G and Gag-Pol vectors for retroviruses. All lentiviral stable cells lines were generated using psPAX2 and pMD2.G vectors. Sin3B-FLAG, and all Sin3B-FLAG truncation mutants were cloned in the pcDNA3.1+ construct. Sin3B-FLAG point mutants were cloned in pcDNA3.1+ for transient transfection and pBABE-puro for retroviral transduction. The following constructs were used for stable transduction: pTRIPZ-EMI1-FLAG Puromycin, pBABE V5-LIN37 Hygromycin (Litovchick et al., 2007), pFUCCI-G_1 Orange MaRX IVf hygro, and pFUCCI-S/G_2/M Green pLB(N)CX Blasticidin. The following constructs were used for transient transfection: LIN9-V5 HIS pEF, LIN37-V5 HIS pEF, p107-HA pCMV, MYC-FOXM1, p130-HA pcDNA3.1+, and BMYB-V5 pcDNA3.1+. A pTRIPZ Puromycin lentiviral doxycycline-inducible short hairpin against human Sin3B was purchased from Dharmacon, V3THS_315587 (AGGCTGTAGACATCGTCCA).

Antibodies—The following antibodies were used for immunoblotting: mouse anti-Sin3B (Santa Cruz H-4 SC-13145), mouse anti-Sin3B (Santa Cruz H-5 SC-55516), rabbit anti-Sin3B (Santa Cruz AK-12), rabbit anti-Sin3A (Santa Cruz K-20), rabbit anti-KI67 (Millipore (Upstate) AB9260), mouse anti-a-tubulin (Sigma-Aldrich T9026), mouse anti-vinculin (Sigma Clone V9131), rabbit anti-vinculin (Cell Signaling 13901), rabbit anti-MYBL2 (Santa Cruz SC-724 N-19), mouse anti-p130 (BD Transduction Labs 610262), rabbit anti-p130 (Santa Cruz C-20 SC-317), mouse anti-CCND1 (Millipore/Calbiochem CC12), rabbit anti-CDKN1B (p27KIP1) (Cell Signaling 2552), rabbit anti-CCNA2 (Santa Cruz C-19 SC-596), mouse anti-CCNE1 (Santa Cruz HE12 SC247), rabbit anti-CCNF (Santa Cruz C-20 SC952), rabbit anti-CDKN1A (p21CIP1) (Santa Cruz C-19), mouse anti-GAPDH (Millipore MAB374), mouse anti-FLAG (M2 Sigma), mouse anti-HA (Sigma 12CA5), mouse anti-MYC tag (Cell Signaling 9B11), rabbit anti-HDAC1 (Cell Signaling D5C6VXP), rabbit anti-HDAC3 (Cell Sigaling #2632), and mouse anti-V5 (Invitrogen). The following antibodies were used for immunoprecipitation: rabbit IgG (Bethyl P120-101), rabbit anti-V5 (Bethyl A190-120-A), mouse anti-HA (Santa Cruz 7392), mouse anti-Sin3B (Santa Cruz H-4 SC-13145), mouse anti-V5 (Invitrogen), and mouse anti-FLAG EZview Red ANTI-FLAG M2 Affinity Gel (Sigma F2426). Rabbit antibodies against LIN9 and LIN37 used for immunoprecipitation and western blots were prepared by Bethyl and previously descibed (Litovchick et al., 2007).

Mass spectrometry—Nuclear extracts were prepared from cells stably expressing Sin3B-FLAG and various Sin3B-FLAG mutants, and incubated with EZview Red ANTI-FLAG M2 affinity gels overnight. Proteins were competitively eluted via Flag peptide and standard binding partner characterization was performed using the Orbitrap Fusion mass spectrometer to acquire high resolution MS and MS/MS spectra of eluted peptides. These data were then searched against the Uniprot mouse database using Sequest in order to generate a list of peptide interactors.

Nuclear lysate extraction—Nuclei were extracted by quick lysis in RSB-G40 lysis buffer (10mM Tris 7.4, 10mM NaCl, 3 mM $MgCl_2$, 10% glycerol, 0.25% NP-40, 0.5 mM DTT, 25 mM NaF, 1 mM sodium orthovanadate, 1 mM PMSF, and cOmplete protease inhibitor cocktail (Sigma)). Nuclei were washed with RSB-G40 without NP-40, and lysed with high-salt extraction buffer (20 mM HEPES pH7.9, 420mM NaCl, 1.5 mM $MgCl_2$, 0.2 mM EDTA, 25% glycerol, 0.5 mM DTT, 25 mM NaF, 1 mM sodium orthovanadate, 1 mM PMSF, and cOmplete protease inhibitor cocktail (Sigma)). Salt concentrations were adjusted with the addition of binding buffer (20mM HEPES pH7.9, 5 mM $MgCl_2$, 10% glycerol, 0.1% Tween-20, 0.5 mM DTT, 25 mM NaF, 1 mM sodium orthovanadate, 1 mM PMSF, and cOmplete protease inhibitor cocktail (Sigma)), and lysates were subjected to either electrophoresis or immunoprecipiation.

Transient transfection co-immunoprecipitations—HEK293T, T98G, or NIH 3T3 cells were transfected with 10 μg of the indicated constructions using a 4:1 ratio of polyethyleneimine (PEI). Cells were incubated for 48 hr, harvested and lysed with 1x EBC buffer (120 mM NaCl, 0.5% v/v NP-40, 50 mM Tris-HCl pH 8.0, 0.01% 2-Mercaptoethanol, 25 mM NaF, 1 mM sodium orthovanadate, 1 mM PMSF, and cOmplete protease inhibitor cocktail (Sigma)). Lysates were incubated with equilibrated mouse anti-FLAG EZview Red ANTI-FLAG M2 Affinity Gel (Sigma F2426) overnight at 4°C with gentle rotation. Beads were washed and protein was eluted via boiling in Laemmli buffer (2x Laemmli buffer: 4% w/v SDS, 20% v/v glycerol, 120 mM Tris-HCl pH 6.8). Eluted lysates were subjected to electrophoresis followed by immunoblotting.

Endogenous and semi-endogenous immunoprecipitations—T98G or NIH 3T3 cells transfected or stably infected with the indicated constructs were harvested on ice and lysed in EBC buffer (50 mM TRIS-HCl pH 8.0, 150 mM NaCl, 0.5% NP-40, 0.5 mM EDTA) (Litovchick et al., 2007) supplemented with 0.01% 2-mercaptoethanol, protease inhibitors (EMD; Cat#539131, Cocktail Set-I) and phosphatase inhibitors (EMD; Cat#524625, Cocktail Set-II). Protein concentrations were measured using DC protein assay kit (Bio-Rad), lysates were normalized and immunoprecipitated with the indicated antibodies (1 μg/ml) using Protein A Sepharose CL-4B Beads (GE Healthcare).

Immunoblot analysis—Cells were lysed in 1x RIPA buffer (1% NP-40, 0.1% SDS, 50 mM Tris-HCl, pH 7.4, 150 mM NaCl, 0.5% sodium deoxycholate, 1 mM EDTA) for whole cell extracts, or 1x EBC buffer (120 mM NaCl, 0.5% v/v NP-40, 50 mM Tris-HCl pH 8.0) for immunoprecipitations, 0.5 μM DTT (0.01% 2-Mercaptoethanol for EBC buffer), 25 mM NaF, 1 mM sodium orthovanadate, 1 mM PMSF, and cOmplete protease inhibitor cocktail

(Sigma). PVDF membranes were blocked in 5% milk/0.1% Tween 20 TBS for 1 hr at room temperature. Primary antibodies were incubated overnight at 4°C. After incubation with either the secondary IRDye Alexa Fluor 680 goat antimouse antibody or 800 goat anti-rabbit antibodies (Odyssey), the membranes were visualized with the Odyssey Infrared Imaging System (Li-Cor). Immunoprecipitations: whole cell lysates (10% inputs) and immunoprecipitates were resolved on 4%–15% gradient Criterion gels (BioRad) and transferred to nitrocellulose membranes using semi-dry Transblot SD cell (BioRad). ReliaBLOT kit (Bethyl Labs; WB120) was used for IP/western blotting according to manufacturer's protocol and membranes were probed with indicated antibodies.

KI67 staining—Cells were starved for 72hrs using DMEM (Cellgro) with 0% FBS and 1% Penicillin/Streptomycin (Cellgro) at < 100% confluency. Cells were then fixed in 70% ethanol, added dropwise while vortexing, at 4°C overnight. Staining was performed overnight at 4°C in the dark using 200,000 cells in 100 μL 1% BSA/PBS using 1 μL anti-mouse KI67 APC (Biolegend 16A8) or 1 uL rat anti-IgG2a κ Isotype control APC (Biolegend RTK2758). Cells were stained using 10 μg/mL Hoechst in 200 μL PBS at room temperature for 10 mins, filtered, and analyzed via flow cytometry using a FACSCalibur Flow Cytometer (BD). A minimum of 30,000 events were counted for each sample.

BrDU staining—Cells were starved for 72hrs using DMEM (Cellgro) with 0% FBS and 1% Penicillin/Streptomycin (Cellgro) at < 100% confluency. Cells were pulsed with 30 μM BrDU for 2 hours. Cells were then fixed in 70% ethanol, added drop wise while vortexing, at 4°C overnight. Chromatin was exposed via 2N HCL and 0.5% Triton X-100, added drop wise while vortexing, at room temperature for 30 mins. HCL was neutralized via 30 min incubation at room temperature with 0.1 M sodium tetraborate ($Na_2B_4O_7 \cdot 10\ H_2O$), pH 8.5.200,000 cells were stained with 1 μL anti-BrDU FITC (BD PharMingen) in 100 μL 0.5% Tween 20/1% BSA/PBS for 30 mins in the dark at room temperature. Cells were then stained with 100 μg/mL propidium iodide, filtered and analyzed via flow cytometry using a FACSCalibur Flow Cytometer (BD). A minimum of 30,000 events were counted for each sample.

Propidium iodide staining—Cells were starved for 72hrs using DMEM (Cellgro) with 0% FBS and 1% Penicillin/Streptomycin (Cellgro) at < 100% confluency. Cells were restimulated with 10% serum for the 0, 10 and 18 hours and fixed in 70% ethanol, added drop wise while vortexing, at 4°C overnight. Cells were washed twice with PBS and stained overnight at 4°C using 100 μg/mL propidium iodide. Cells were filtered and analyzed via flow cytometry using a FACSCalibur Flow Cytometer (BD). A minimum of 30,000 events were counted for each sample.

Chromatin Immunoprecipitation (ChIP)—Cells were serum starved for 72 hours and lyzed in the presence of Trichostatin A and protease inhibitors. ChIP was performed as previously (DiMauro et al., 2015; Grandinetti et al., 2009) using 750 μg proteins from whole cell extractswith 2 μg of the following antibodies. Sin3B (SCBT, H4); H3 (Abcam, ab17911), acK9-H3 (EMD Millipore, 06-942), E2F4 (SCBT, D7), and c-kit (SCBT, M14). qRT-PCR was performed using primers previously described (Müller et al., 2016).

RNA preparation for sequencing—Cells were starved for 72hrs using DMEM (Cellgro) with 0% FBS and 1% Penicillin/Streptomycin (Cellgro) at < 100% confluency. Cells were restimulated with 10% serum for the 0, 10 and 18 hours and harvested for RNA. RNA was extracted via column purification using RNeasy Mini Kit (QIAGEN).

QUANTIFICATION AND STATISTICAL ANALYSIS

Statistics—All data were analyzed by Student's t test (unpaired, 2-tailed) and results were considered significant at $p < 0.05$. Results are presented as mean ± SEM.

RNA sequencing—Raw reads were trimmed by performing a sliding window trimming using Trimmomatic (version 0.33) with a window size of 4 and quality threshold of 10 (Bolger et al., 2014). Reads were aligned to the genome using Tophat (version 2.1.1) with default settings (Trapnell et al., 2012). For each gene, read counts were assigned using HTSeq-count. To determine differential expression between experiment and control groups, the edgeR statistical package was used and the generalized linear model likelihood ratio test applied using the function glmLRT() (Robinson et al., 2010). Differentially expressed genes were determined as genes with false discovery rate < 0.1.

DATA AND SOFTWARE AVAILABILITY

The accession numbers for the sequencing data reported in this paper are on GEO repository GSE121857 and can be accessed at https://www.ncbi.nlm.nih.gov/geo/query/acc.cgi?acc=GSE121857.

Supplementary Material

Refer to Web version on PubMed Central for supplementary material.

ACKNOWLEDGMENTS

We thank all of the members of the David laboratory for helpful discussions during the preparation of this manuscript. We wish to acknowledge the NYU Proteomics Laboratory (supported in part by Laura and Isaac Perlmutter Cancer Center Support Grant NIH/NCI P30CA016087) for help with mass spectrometry analysis and the NYU Genome Technology Center (supported in part by Laura and Isaac Perlmutter Cancer Center Support Grant NIH/NCI P30CA016087) for help with RNA sequencing (RNA-seq) experiments. We thank Dr. Michele Pagano (NYU School of Medicine) and Dr. J.A. DeCaprio (Dana Farber Cancer Institute) for the generous gift of various reagents. Finally, we thank Dr. Tony Huang (NYU School of Medicine), Dr. Michele Pagano (NYU School of Medicine), Ishwar Radhakrishnan (Northwestern University), and Dr. Julien Sage (Stanford University) for helpful discussions. This work was funded by NIH/NCI R01CA148639 and R21CA155736 (G.D.), R01CA188571 (L.L.), the Samuel Waxman Cancer Research Foundation (G.D.), and a pilot grant from the NYU Department of Urology (G.D.). A.J.B. was supported by a predoctoral NIH/NIGMS training grant (T32GM066704) (E.A. Bach); D.J.C. was supported by a predoctoral NIH/NCI training grant (T32CA009161) (D.E. Levy) and a predoctoral NIH/NCI NRSA grant (F30CA203047).

REFERENCES

Anders S, Pyl PT, and Huber W (2015). HTSeq—a Python framework to work with high-throughput sequencing data. Bioinformatics 31, 166–169. [PubMed: 25260700]

Bainor AJ, Deng FM, Wang Y, Lee P, Cantor DJ, Logan SK, and David G (2017). Chromatin-associated protein SIN3B prevents prostate cancer progression by inducing senescence. Cancer Res. 77, 5339–5348. [PubMed: 28807943]

Balciunaite E, Spektor A, Lents NH, Cam H, Te Riele H, Scime A, Rudnicki MA, Young R, and Dynlacht BD (2005). Pocket protein complexes are recruited to distinct targets in quiescent and proliferating cells. Mol. Cell. Biol. 25, 8166–8178. [PubMed: 16135806]

Bansal N, David G, Farias E, and Waxman S (2016). Emerging roles of epigenetic regulator Sin3 in cancer. Adv. Cancer Res. 130, 113–135. [PubMed: 27037752]

Bartke T, Vermeulen M, Xhemalce B, Robson SC, Mann M, and Kouzarides T (2010). Nucleosome-interacting proteins regulated by DNA and histone methylation. Cell 143, 470–484. [PubMed: 21029866]

Beijersbergen RL, Hijmans EM, Zhu L, and Bernards R (1994). Interaction of c-Myc with the pRb-related protein p107 results in inhibition of c-Myc-mediated transactivation. EMBO J. 13, 4080–4086. [PubMed: 8076603]

Bolger AM, Lohse M, and Usadel B (2014). Trimmomatic: a flexible trimmer for Illumina sequence data. Bioinformatics 30, 2114–2120. [PubMed: 24695404]

Cantor DJ, and David G (2017). The chromatin-associated Sin3B protein is required for hematopoietic stem cell functions in mice. Blood 129, 60–70. [PubMed: 27806947]

Chen EY, Tan CM, Kou Y, Duan Q, Wang Z, Meirelles GV, Clark NR, and Ma'ayan A (2013). Enrichr: interactive and collaborative HTML5 gene list enrichment analysis tool. BMC Bioinformatics 14, 128. [PubMed: 23586463]

Dannenberg JH, van Rossum A, Schuijff L, and te Riele H (2000). Ablation of the retinoblastoma gene family deregulates G(1) control causing immortalization and increased cell turnover under growth-restricting conditions. Genes Dev. 14, 3051–3064. [PubMed: 11114893]

Dannenberg JH, David G, Zhong S, van der Torre J, Wong WH, and Depinho RA (2005). mSin3A corepressor regulates diverse transcriptional networks governing normal and neoplastic growth and survival. Genes Dev. 19, 1581–1595. [PubMed: 15998811]

David G, Grandinetti KB, Finnerty PM, Simpson N, Chu GC, and Depinho RA (2008). Specific requirement of the chromatin modifier mSin3B in cell cycle exit and cellular differentiation. Proc. Natl. Acad. Sci. USA 105, 4168–4172. [PubMed: 18332431]

DiMauro T, Cantor DJ, Bainor AJ, and David G (2015). Transcriptional repression of Sin3B by Bmi-1 prevents cellular senescence and is relieved by oncogene activation. Oncogene 34, 4011–4017. [PubMed: 25263442]

Dimova DK, and Dyson NJ (2005). The E2F transcriptional network: old acquaintances with new faces. Oncogene 24, 2810–2826. [PubMed: 15838517]

Dyson N, Dembski M, Fattaey A, Ngwu C, Ewen M, and Helin K (1993). Analysis of p107-associated proteins: p107 associates with a form of E2F that differs from pRB-associated E2F-1. J. Virol. 67, 7641–7647. [PubMed: 8230483]

Eng JK, McCormack AL, and Yates JR (1994). An approach to correlate tandem mass spectral data of peptides with amino acid sequences in a protein database. J. Am. Soc. Mass Spectrom. 5, 976–989. [PubMed: 24226387]

Fay DS, Keenan S, and Han M (2002). fzr-1 and lin-35/Rb function redundantly to control cell proliferation in *C. elegans* as revealed by a nonbiased synthetic screen. Genes Dev. 16, 503–517. [PubMed: 11850412]

Fischer M, Grossmann P, Padi M, and DeCaprio JA (2016). Integration of TP53, DREAM, MMB-FOXM1 and RB-E2F target gene analyses identifies cell cycle gene regulatory networks. Nucleic Acids Res. 44, 6070–6086. [PubMed: 27280975]

Forristal C, Henley SA, MacDonald JI, Bush JR, Ort C, Passos DT, Talluri S, Ishak CA, Thwaites MJ, Norley CJ, et al. (2014). Loss of the mammalian DREAM complex deregulates chondrocyte proliferation. Mol. Cell. Biol. 34, 2221–2234. [PubMed: 24710275]

Ginsberg D, Vairo G, Chittenden T, Xiao ZX, Xu G, Wydner KL, De-Caprio JA, Lawrence JB, and Livingston DM (1994). E2F-4, a new member of the E2F transcription factor family, interacts with p107. Genes Dev. 8, 2665–2679. [PubMed: 7958924]

Grandinetti KB, Jelinic P, DiMauro T, Pellegrino J, Fernández Rodríguez R, Finnerty PM, Ruoff R, Bardeesy N, Logan SK, and David G (2009). Sin3B expression is required for cellular senescence and is up-regulated upon oncogenic stress. Cancer Res. 69, 6430–6437. [PubMed: 19654306]

Graveline R, Marcinkiewicz K, Choi S, Paquet M, Wurst W, Floss T, and David G (2017). The chromatin-associated Phf12 protein maintains nucleolar integrity and prevents premature cellular senescence. Mol. Cell. Biol. 37, e00522–s16. [PubMed: 27956701]

Guiley KZ, Liban TJ, Felthousen JG, Ramanan P, Litovchick L, and Rubin SM (2015). Structural mechanisms of DREAM complex assembly and regulation. Genes Dev. 29, 961–974. [PubMed: 25917549]

Harrison MM, Ceol CJ, Lu X, and Horvitz HR (2006). Some C. elegans class B synthetic multivulva proteins encode a conserved LIN-35 Rb-containing complex distinct from a NuRD-like complex. Proc. Natl. Acad. Sci. USA 103, 16782–16787. [PubMed: 17075059]

Hassig CA, Fleischer TC, Billin AN, Schreiber SL, and Ayer DE (1997). Histone deacetylase activity is required for full transcriptional repression by mSin3A. Cell 89, 341–347. [PubMed: 9150133]

Hayakawa T, Ohtani Y, Hayakawa N, Shinmyozu K, Saito M, Ishikawa F, and Nakayama J (2007). RBP2 is an MRG15 complex component and down-regulates intragenic histone H3 lysine 4 methylation. Genes Cells 12, 811–826. [PubMed: 17573780]

Heinzel T, Lavinsky RM, Mullen TM, Söderstrom M, Laherty CD, Torchia J, Yang WM, Brard G, Ngo SD, Davie JR, et al. (1997). A complex containing N-CoR, mSin3 and histone deacetylase mediates transcriptional repression. Nature 387, 43–48. [PubMed: 9139820]

Jelinic P, Pellegrino J, and David G (2011). A novel mammalian complex containing Sin3B mitigates histone acetylation and RNA polymerase II progression within transcribed loci. Mol. Cell. Biol. 31, 54–62. [PubMed: 21041482]

Kuleshov MV, Jones MR, Rouillard AD, Fernandez NF, Duan Q, Wang Z, Koplev S, Jenkins SL, Jagodnik KM, Lachmann A, et al. (2016). Enrichr: a comprehensive gene set enrichment analysis web server 2016 update. Nucleic Acids Res. 44 (W1), W90–W97. [PubMed: 27141961]

Lai A, Kennedy BK, Barbie DA, Bertos NR, Yang XJ, Theberge MC, Tsai SC, Seto E, Zhang Y, Kuzmichev A, et al. (2001). RBP1 recruits the mSIN3-histone deacetylase complex to the pocket of retinoblastoma tumor suppressor family proteins found in limited discrete regions of the nucleus at growth arrest. Mol. Cell. Biol. 21, 2918–2932. [PubMed: 11283269]

Lees JA, Saito M, Vidal M, Valentine M, Look T, Harlow E, Dyson N, and Helin K (1993). The retinoblastoma protein binds to a family of E2F transcription factors. Mol. Cell. Biol. 13, 7813–7825. [PubMed: 8246996]

Litovchick L, Sadasivam S, Florens L, Zhu X, Swanson SK, Velmurugan S, Chen R, Washburn MP, Liu XS, and DeCaprio JA (2007). Evolutionarily conserved multisubunit RBL2/p130 and E2F4 protein complex represses human cell cycle-dependent genes in quiescence. Mol. Cell 26, 539–551. [PubMed: 17531812]

Litovchick L, Florens LA, Swanson SK, Washburn MP, and DeCaprio JA (2011). DYRK1A protein kinase promotes quiescence and senescence through DREAM complex assembly. Genes Dev. 25, 801–813. [PubMed: 21498570]

Mages CF, Wintsche A, Bernhart SH, and Müller GA (2017). The DREAM complex through its subunit Lin37 cooperates with Rb to initiate quiescence. eLife 6, e26876. [PubMed: 28920576]

Malovannaya A, Lanz RB, Jung SY, Bulynko Y, Le NT, Chan DW, Ding C, Shi Y, Yucer N, Krenciute G, et al. (2011). Analysis of the human endogenous coregulator complexome. Cell 145, 787–799. [PubMed: 21620140]

Müller GA, Stangner K, Schmitt T, Wintsche A, and Engeland K (2016). Timing of transcription during the cell cycle: protein complexes binding to E2F, E2F/CLE, CDE/CHR, or CHR promoter elements define early and late cell cycle gene expression. Oncotarget 8, 97736–97748. [PubMed: 29228647]

Odajima J, Saini S, Jung P, Ndassa-Colday Y, Ficaro S, Geng Y, Marco E, Michowski W, Wang YE, DeCaprio JA, et al. (2016). Proteomic landscape of tissue-specific cyclin E functions in vivo. PLoS Genet. 12, e1006429. [PubMed: 27828963]

Osterloh L, von Eyss B, Schmit F, Rein L, Hübner D, Samans B, Hauser S, and Gaubatz S (2007). The human synMuv-like protein LIN-9 is required for transcription of G2/M genes and for entry into mitosis. EMBO J. 26, 144–157. [PubMed: 17159899]

Pilkinton M, Sandoval R, and Colamonici OR (2007). Mammalian Mip/LIN-9 interacts with either the p107, p130/E2F4 repressor complex or B-Myb in a cell cycle-phase-dependent context distinct from the *Drosophila* dREAM complex. Oncogene 26, 7535–7543. [PubMed: 17563750]

Rayman JB, Takahashi Y, Indjeian VB, Dannenberg JH, Catchpole S, Watson RJ, te Riele H, and Dynlacht BD (2002). E2F mediates cell cycledependent transcriptional repression in vivo by recruitment of an HDAC1/mSin3B corepressor complex. Genes Dev. 16, 933–947. [PubMed: 11959842]

Reimann JD, Freed E, Hsu JY, Kramer ER, Peters JM, and Jackson PK (2001). Emi1 is a mitotic regulator that interacts with Cdc20 and inhibits the anaphase promoting complex. Cell 105, 645–655. [PubMed: 11389834]

Rielland M, Cantor DJ, Graveline R, Hajdu C, Mara L, Diaz Bde.D., Miller G, and David G (2014). Senescence-associated SIN3B promotes inflammation and pancreatic cancer progression. J. Clin. Invest. 124, 2125–2135. [PubMed: 24691445]

Robinson MD, McCarthy DJ, and Smyth GK (2010). edgeR: a Bioconductor package for differential expression analysis of digital gene expression data. Bioinformatics 26, 139–140. [PubMed: 19910308]

Sadasivam S, and DeCaprio JA (2013). The DREAM complex: master coordinator of cell cycle-dependent gene expression. Nat. Rev. Cancer 13, 585–595. [PubMed: 23842645]

Sadasivam S, Duan S, and DeCaprio JA (2012). The MuvB complex sequentially recruits B-Myb and FoxM1 to promote mitotic gene expression. Genes Dev. 26, 474–489. [PubMed: 22391450]

Sage J, Miller AL, Pérez-Mancera PA, Wysocki JM, and Jacks T (2003). Acute mutation of retinoblastoma gene function is sufficient for cell cycle re-entry. Nature 424, 223–228. [PubMed: 12853964]

Sakaue-Sawano A, Kurokawa H, Morimura T, Hanyu A, Hama H, Osawa H, Kashiwagi S, Fukami K, Miyata T, Miyoshi H, et al. (2008). Visualizing spatiotemporal dynamics of multicellular cell-cycle progression. Cell 132, 487–498. [PubMed: 18267078]

Sandoval R, Pilkinton M, and Colamonici OR (2009). Deletion of the p107/p130-binding domain of Mip130/LIN-9 bypasses the requirement for CDK4 activity for the dissociation of Mip130/LIN-9 from p107/p130-E2F4 complex. Exp. Cell Res. 315, 2914–2920. [PubMed: 19619530]

Saville MK, and Watson RJ (1998). The cell-cycle regulated transcription factor B-Myb is phosphorylated by cyclin A/Cdk2 at sites that enhance its transactivation properties. Oncogene 17, 2679–2689. [PubMed: 9840932]

Schmit F, Korenjak M, Mannefeld M, Schmitt K, Franke C, von Eyss B, Gagrica S, Hänel F, Brehm A, and Gaubatz S (2007). LINC, a human complex that is related to pRB-containing complexes in invertebrates regulates the expression of G2/M genes. Cell Cycle 6, 1903–1913. [PubMed: 17671431]

Silverstein RA, and Ekwall K (2004). Sin3: a flexible regulator of global gene expression and genome stability. Curr. Genet 47, 1–17. [PubMed: 15565322]

Solari F, and Ahringer J (2000). NURD-complex genes antagonise Ras-induced vulval development in Caenorhabditis elegans. Curr. Biol. 10, 223–226. [PubMed: 10704416]

Subramanian A, Tamayo P, Mootha VK, Mukherjee S, Ebert BL, Gillette MA, Paulovich A, Pomeroy SL, Golub TR, Lander ES, and Mesirov JP (2005). Gene set enrichment analysis: a knowledge-based approach for interpreting genome-wide expression profiles. Proc. Natl. Acad. Sci. USA 102, 15545–15550. [PubMed: 16199517]

Tedesco D, Lukas J, and Reed SI (2002). The pRb-related protein p130 is regulated by phosphorylation-dependent proteolysis via the protein-ubiquitin ligase SCF(Skp2). Genes Dev. 16, 2946–2957. [PubMed: 12435635]

Trapnell C, Pachter L, and Salzberg SL (2009). TopHat: discovering splice junctions with RNA-Seq. Bioinformatics 25, 1105–1111. [PubMed: 19289445]

Trapnell C, Roberts A, Goff L, Pertea G, Kim D, Kelley DR, Pimentel H, Salzberg SL, Rinn JL, and Pachter L (2012). Differential gene and transcript expression analysis of RNA-seq experiments with TopHat and Cufflinks. Nat. Protoc. 7, 562–578. [PubMed: 22383036]

Tschöp K, Conery AR, Litovchick L, Decaprio JA, Settleman J, Harlow E, and Dyson N (2011). A kinase shRNA screen links LATS2 and the pRB tumor suppressor. Genes Dev. 25, 814–830. [PubMed: 21498571]

Vairo G, Livingston DM, and Ginsberg D (1995). Functional interaction between E2F-4 and p130: evidence for distinct mechanisms underlying growth suppression by different retinoblastoma protein family members. Genes Dev. 9, 869–881. [PubMed: 7705662]

van Oevelen C, Wang J, Asp P, Yan Q, Kaelin WG, Jr., Kluger Y, and Dynlacht BD (2008). A role for mammalian Sin3 in permanent gene silencing. Mol. Cell 32, 359–370. [PubMed: 18995834]

van Oevelen C, Bowman C, Pellegrino J, Asp P, Cheng J, Parisi F, Micsinai M, Kluger Y, Chu A, Blais A, et al. (2010). The mammalian Sin3 proteins are required for muscle development and sarcomere specification. Mol. Cell. Biol. 30, 5686–5697. [PubMed: 20956564]

Zhang Y, Iratni R, Erdjument-Bromage H, Tempst P, and Reinberg D (1997). Histone deacetylases and SAP18, a novel polypeptide, are components of a human Sin3 complex. Cell 89, 357–364. [PubMed: 9150135]

Highlights

- The chromatin modifier Sin3B interacts with the DREAM complex
- Sin3B is required for the repression of DREAM target genes in quiescence
- Sin3B inactivation allows quiescent cells to enter S phase upon APC/C^{CDH1} inhibition

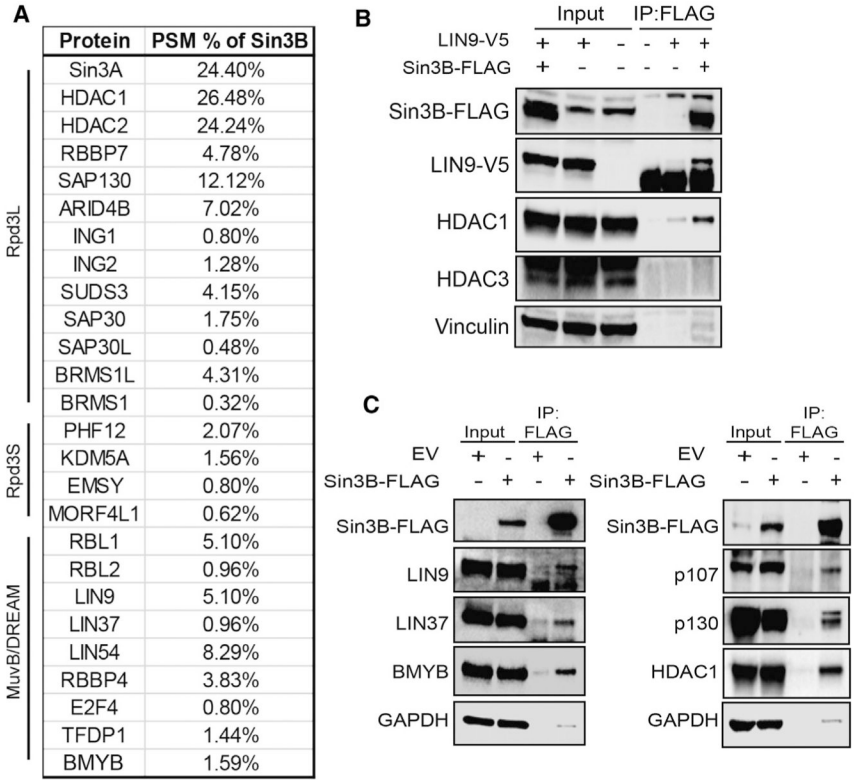

Figure 1. Identification of Sin3B's Canonical and Additional Interactors

(A) Normalized peptide-spectrum match (PSM) values of canonical and additional interactors. PSM % is the PSM value of each protein normalized to Sin3B signal, related as a percentage. RPD3L, large Sin3 complex; RPD3S, small Sin3 complex.

(B) Co-immunoprecipitations with an anti-FLAG antibody of whole-cell extracts from T98G cells transfected with the indicated plasmids. Immunoblots were performed using the indicated antibodies. 10% input. IP, immunoprecipitation.

(C) Co-immunoprecipitations with an anti-FLAG antibody of whole-cell extracts from T98G cells transiently transfected with Sin3B-FLAG or empty vector (EV). Immunoblots were performed using the indicated antibodies. 10% input. IP, immunoprecipitation.

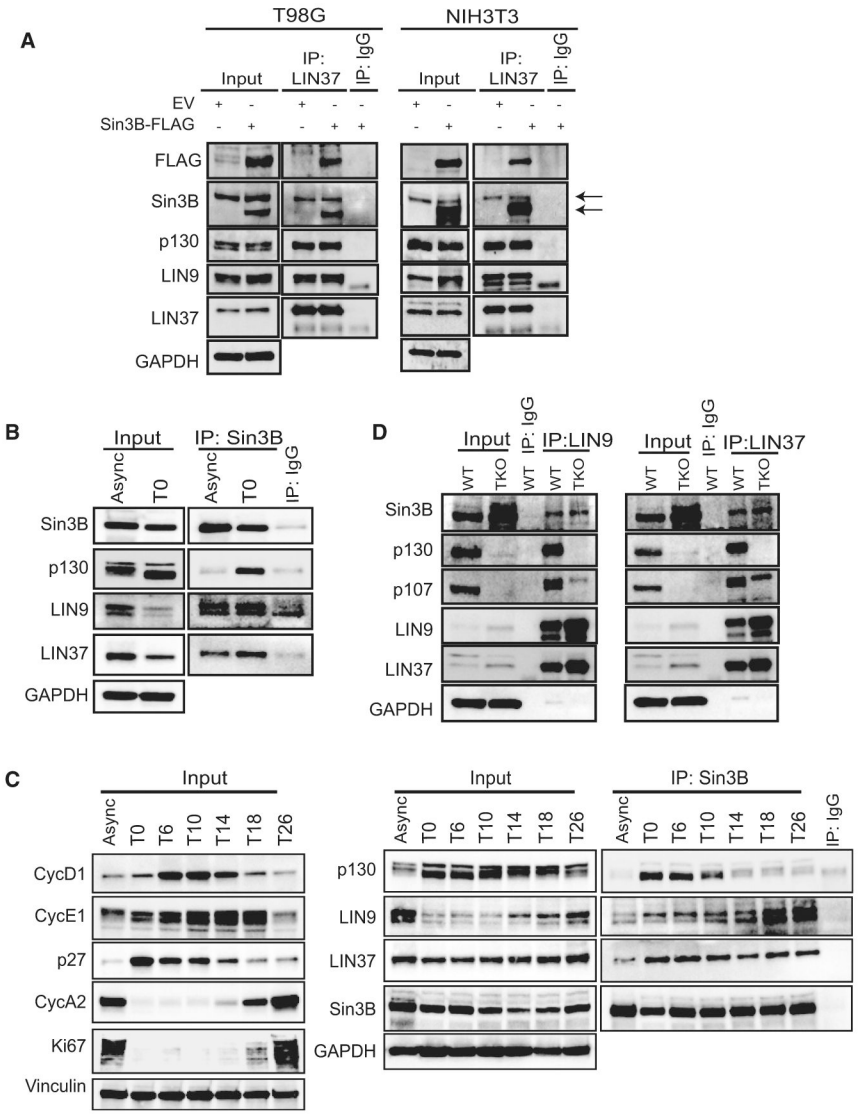

Figure 2. Sin3B Interacts with the DREAM Complex

(A) Co-immunoprecipitation using an anti-LIN37 antibody of whole-cell extracts from human T98G cells (left) or mouse NIH 3T3 cells (right) transiently transfected with Sin3B-FLAG or empty vector (EV). Immunoblots were performed using the indicated antibodies. 10% input. IP, immunoprecipitation. Top arrow, endogenous Sin3B; bottom arrow, exogenous Sin3B. IgG, immunoglobulin G.

(B) Co-immunoprecipitation on endogenous proteins using an anti-Sin3B antibody of whole-cell extracts from T98G cells either asynchronously growing (Async) or serum starved for 72 hr (T0). Immunoblots were performed using the indicated antibodies. 10% input. IP, immunoprecipitation; IgG, immunoglobulin G.

(C) Left panels: western blot of whole-cell extracts from T98G cells asynchronously growing (Async), serum starved for 72 hr (T0), and serum starved for 72 hr and released for 6–26 hr (T6 to T26) with the indicated antibodies. Right panel: co-immunoprecipitation on

endogenous proteins using an anti-Sin3B antibody of same whole-cell extracts. 10% input. IP, immunoprecipitation; IgG, immunoglobulin G.

(D) Co-immunoprecipitation on endogenous proteins using an anti-Lin9 antibody (left panel) or Lin37 antibody (right panel) from growing NIH 3T3 (wild-type [WT]) or Rb-p107-p130 triple knockout spontaneously immortalized mouse embryonic fibroblasts (MEFs) (TKO). Immunoblots were performed using the indicated antibodies. 10% input. IP, immunoprecipitation; IgG, immunoglobulin G.

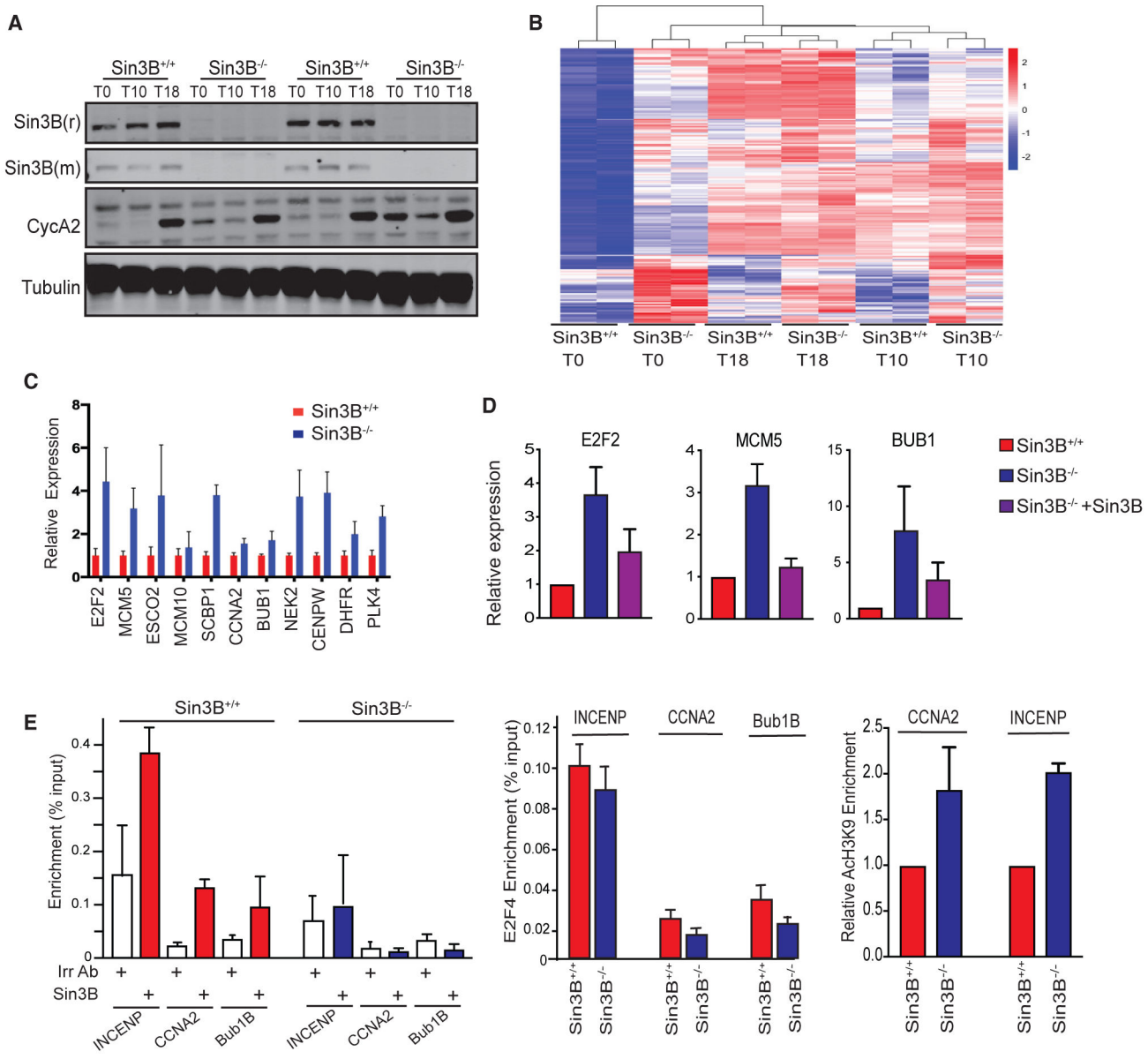

Figure 3. Sin3B Is Required for the Repression of DREAM Target Genes

(A) Western blot on whole-cell lysate from T98G cells of the indicated genotypes 0 (T0), 10 (T10), and 18 hr (T18) post serum addition and probed using the indicated antibodies.

(B) RNA from T98G cells harvested at the indicated time points was used for deep sequencing. Differential gene expression was performed comparing the averaged wild-type and Sin3B-deleted cell lines at T0. A heatmap representing the expression of the 429 significantly de-repressed genes at T0 is shown here at all time points.

(C) qRT-PCR for the indicated DREAM target genes in serum-starved Sin3B$^{+/+}$ and Sin3B$^{-/-}$ T98G. n = 6(3 biological replicates using at least 2 independent cell lines per genotype for each point). Error bars represent SEM.

(D) qRT-PCR for the indicated DREAM target genes in serum-starved Sin3B$^{+/+}$, Sin3B$^{-/-}$, and Sin3B$^{-/-}$ T98G cells stably expressing FLAG-tagged Sin3B (n = 4 biological replicates).

(E) Chromatin immunoprecipitation (ChIP) in serum-starved Sin3B$^{+/+}$ (red bars) and Sin3B$^{-/-}$ (blue bars) T98G cells for Sin3B (left), E2F4 (middle), or AcK9-H3/total H3 (right), at the promoter of the indicated genes. An antibody raised against c-kit is used as control (Irr Ab). Shown is the average of three independent biological replicates, and error bars represent SEM.

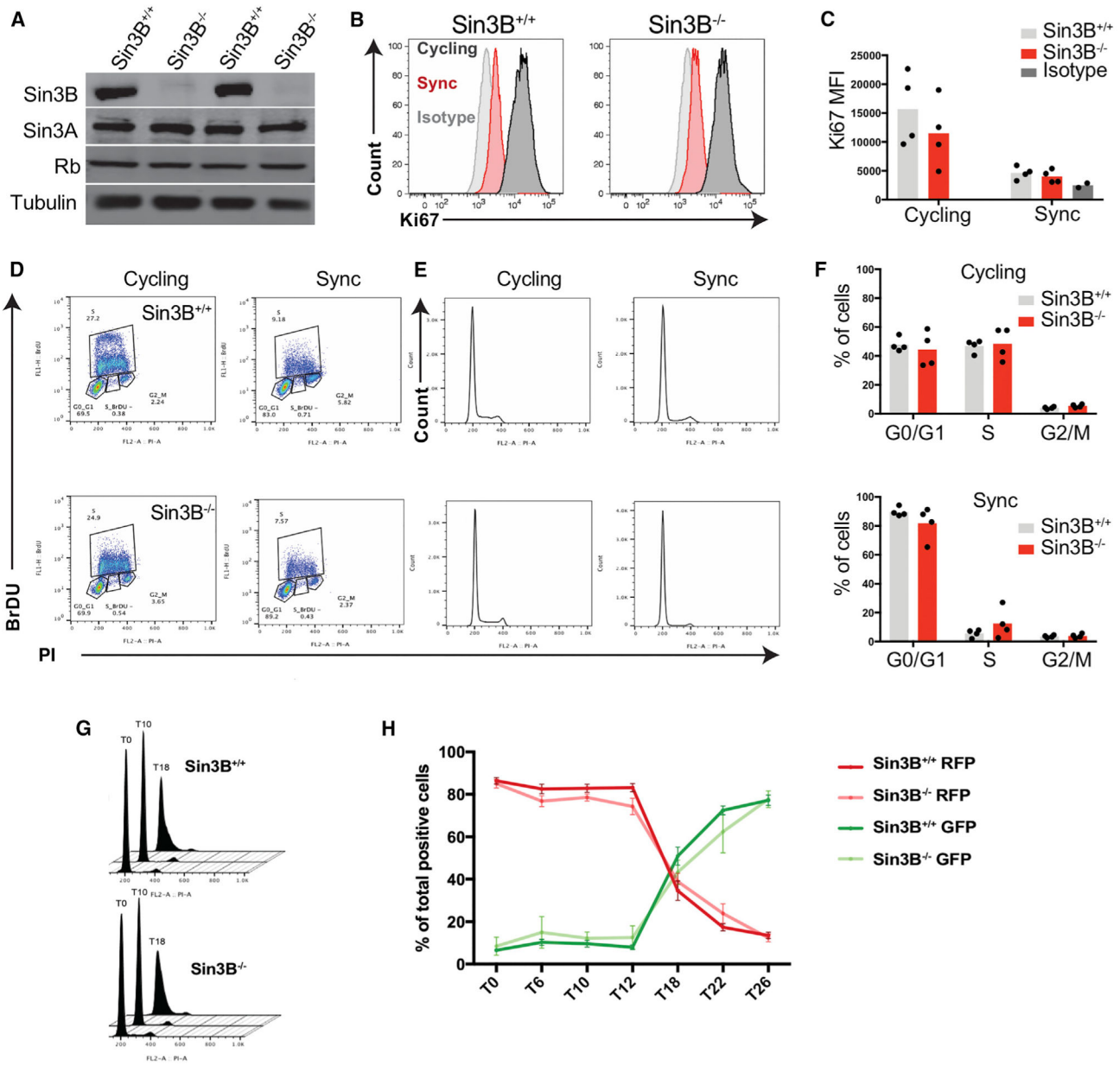

Figure 4. Sin3B Is Not Required for Entry into Quiescence

(A) Western blot for two independent Sin3B wild-type (left) and two independent Sin3B knockout (right) T98G cell lines. Immunoblotting was performed using 40 μg of whole-cell lysates probed using the indicated antibodies.

(B) Representative flow plots of KI67 staining in $Sin3B^{+/+}$ and $Sin3B^{-/-}$ T98G cells. Cells were stained for KI67. Cycling, asynchronous, cycling cells; Sync, serumstarved cells for 72 hr; Isotype, isotype control antibody.

(C) Quantification of KI67 mean fluorescence intensity (MFI) from (A). n = 4 (2 independent cell lines per genotype with 2 experimental replicates each).

(D) Representative flow plots of BrdU staining in $Sin3B^{+/+}$ and $Sin3B^{-/-}$ T98G cells. Cells were starved for 72 hr, pulsed for 2 hr with BrdU, and stained.

(E) Propidium iodide flow plots from (D).

(F) Quantification of (C). n = 4 (2 independent cell lines per genotype with 2 experimental replicates each).

(G) Representative flow plots of PI staining for $Sin3B^{+/+}$ and $Sin3B^{-/-}$ T98G cells, synchronized in G_0 by serum deprivation for 72 hr (T0) or release upon addition of serum for 10 hr (T10) or 18 hr (T18).

(H) $Sin3B^{+/+}$ and $Sin3B^{-/-}$ T98G cells expressing FUCCI probes (RFP, pFUCCI-G_1; GFP, pFUCCI-S/G_2/M) were serum deprived for 72 hr and released into 10% serum for the indicated time, and the amount of RFP and GFP fluorescence was quantified. n = 6 (2 independent cell lines per genotype with 3 technical replicates each).

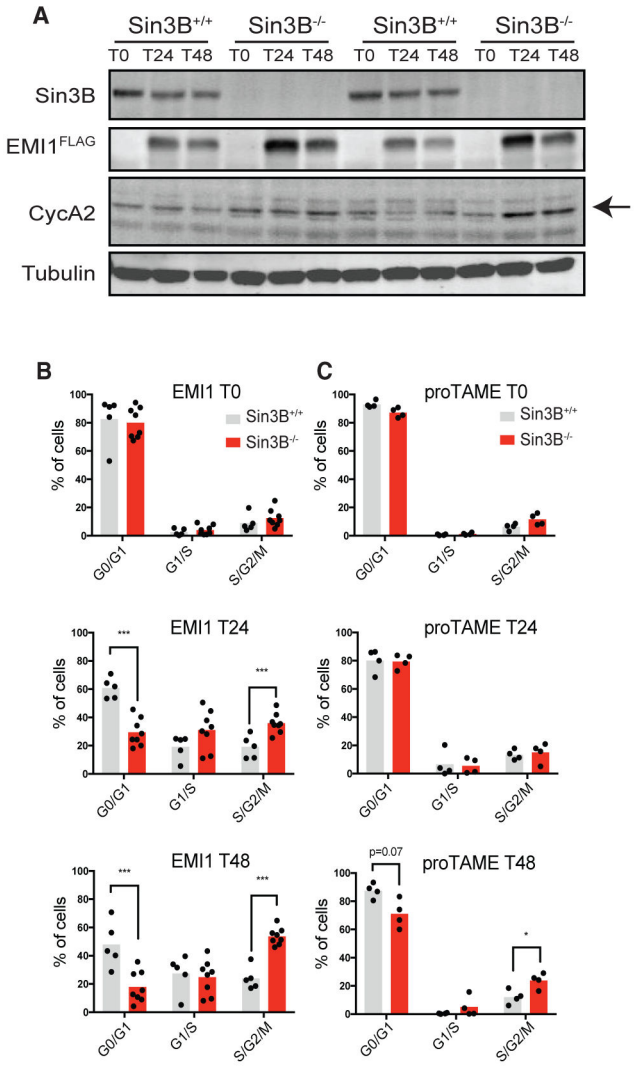

Figure 5. Inhibition of APC/C^{CDH1} Is Sufficient to Cause Quiescent Sin3B-Deleted Cells to Re-enter the Cell Cycle

(A) Immunoblots with the indicated antibodies of whole-cell lysate from two independent Sin3B$^{+/+}$ and two independent Sin3B$^{-/-}$ T98G serum-starved cell lines infected with a doxycycline-inducible Emi1 expression vector. Cells were kept in no-serum conditions and doxycycline was added for 24 hr(T24) or 48 hr (T48).

(B) FUCCI-expressing T98G cells were serum deprived for 96 hr prior to doxycycline administration to induce EMI1 expression. Positivity for the FUCCI probes was quantified at 24 and 48 hr post doxycycline addition. Cells expressing Cdt1-RFP were counted as in G_0/G_1 phase, cells expressing geminin1-GFP as in $S/G_2/M$ phases, and cells expressing both Cdt1-RFP and gemini1-GFP as in G_1/S. For each condition, at least two independent experiments with each cell line presented in (A) were performed.

(C) FUCCI expressing T98G cells were serum deprived for 96 hr prior to the addition of proTAME. Positivity for the FUCCI probes was quantified at 24 and 48 hr post doxycycline addition to inhibit APC/C^{CDH1} activity. *p < 0.05.

KEY RESOURCES TABLE

REAGENT or RESOURCE	SOURCE	IDENTIFIER
Antibodies		
Mouse monoclonal anti-Sin3B (clone H-4)	Santa Cruz	sc-13145; RRID: AB_628254
Mouse monoclonal anti-Sin3B (clone H-5)	Santa Cruz	sc-55516; RRID: AB_2197789
Rabbit polyclonal anti-Sin3B (AK-12)	Santa Cruz	sc-758
Rabbit polyclonal anti-Sin3A (K-20)	Santa Cruz	sc-994; RRID: AB_2187760
Rabbit polyclonal anti-Ki67	Millipore Sigma	AB9260; RRID: AB_2142366
Mouse monoclonal anti-α-Tubulin (clone DM1A)	Millipore Sigma	T9026; RRID: AB_477593
Mouse monoclonal anti-α-Tubulin (clone DM1A)	Cell Signaling	3873; RRID: AB_1904178
Mouse monoclonal anti-Vinculin (clone hVIN-1)	Millipore Sigma	V9131: RRID: AB_477629
Rabbit monoclonal anti-Vinculin (clone E1E9V)	Cell Signaling	13901; RRID: AB_2728768
Rabbit polyclonal anti-B-Myb (N-19)	Santa Cruz	sc-724; RRID: AB_631985
Mouse monoclonal anti-Rb (clone Rb1)	Santa Cruz	Sc-73598; RRID: AB_1128965
Mouse monoclonal anti-Rb2 (clone 10/Rb2)	BD Transduction Labs	610262; RRID: AB_397657
Rabbit polyclonal anti-p130 (C-20)	Santa Cruz	sc-317; RRID: AB_632093
Mouse monoclonal anti-Cyclin D1 (clone DCS-6)	Millipore Sigma	CC12; RRID: AB_2070408
Rabbit polyclonal anti-p27 Kip1	Cell Signaling	2552; RRID: AB_10693314
Rabbit polyclonal anti-Cyclin A (C-19)	Santa Cruz	sc-596; RRID: AB_631330
Rabbit polyclonal anti-Cyclin A2	M. Pagano (NYU)	N/A
Mouse monoclonal anti-Cyclin E (clone HE12)	Santa Cruz	sc-247; RRID: AB_627357
Rabbit polyclonal anti-Cyclin F (C-20)	Santa Cruz	sc-952; RRID: AB_2071212
Rabbit polyclonal anti-p21 (C-19)	Santa Cruz	sc-397; RRID: AB_632126
Mouse monoclonal anti-GAPDH (clone 6C5)	Millipore Sigma	MAB374; RRID: AB_2107445
Rabbit monoclonal anti-HDAC1 (clone D5C6U)	Cell Signaling	34589
Rabbit polyclonal anti-HDAC3	Cell Signaling	2632; RRID: AB_331545
Rabbit polyclonal anti-Histone H3	Abcam	ab1791; RRID: AB_302613
Rabbit polyclonal anti-αcetyl-Histone H3 (Lys9)	Millipore Sigma	06–942; RRID: AB_310308
Mouse monoclonal anti-E2F4 (clone D7)	Santa Cruz	sc-398543
Goal polyclonal anti-cKit (M-14)	Santa Cruz	sc-1494; RRID: AB_631032
Mouse monoclonal FITC anti-BrdU (clone 3D4)	BioLegend	364103; RRID: AB_2564480
Rat monoclonal APC anti-Ki67 (clone 16A8)	BioLegend	652405; RRID: AB_2561929
Rabbit anti-Lin9	(Litovchick et al., 2007)	N/A
Rabbit anti-Lin37	(Litovchick et al., 2007)	N/A
Mouse monoclonal Anti-FLAG (clone M2)	Millipore Sigma	F1804; RRID: AB_262044
EZview Red ANTI-FLAG tag M2 Affinity Gel	Millipore Sigma	F2426; RRID: AB_2616449
Mouse monoclonal anti-HA tag (clone 12CA5)	Millipore Sigma	SAB1305536; RRID: AB_514505
Mouse monoclonal anti-HA tag (clone F-7)	Santa Cruz	sc-7392; RRID: AB_627809
Mouse monoclonal anti-Myc tag (clone 9B11)	Cell Signaling	2276; RRID: AB_331783
Mouse monoclonal anti-V5 tag	ThermoFisher	R960–25; RRID: AB_2556564
Rabbit polyclonal anti-V5 tag	Bethyl Laboratories	A190–120A; RRID: AB_67586

REAGENT or RESOURCE	SOURCE	IDENTIFIER
Goat polyclonal IRDye 680RD anti-mouse IgG (H+L)	Li-Cor	925–68070; RRID: AB_2651128
Goat polyclonal IRDye 800CW anti-rabbit IgG (H+L)	Li-Cor	925–32211; RRID: AB_2651127
Purified Rat APC IgG2a κ Isotype	BioLegend	400511; RRID: AB_2561754
Purified Rabbit IgG	Bethyl Laboratories	P120–101; RRID: AB_479829
Bacterial and vairus strains		
DH5α (*E. coli*)	New England Biolabs	C2988J
Biological Samples		
N/A	N/A	N/A
Chemicals, Peptides, and Recombinant Proteins		
Fetal Bovine Serum (Premium)	Atlanta Biologicals	S11150
Donor Bovine Serum	Atlanta Biologicals	S11350
FLAG Peptide	Millipore Sigma	F3290
proTAME	Boston Biochem	I-440
Propidium Iodide	Millipore Sigma	P4170
Sodium Orthovanadate (Na_3VO_4)	NEB	P0758S
Sodium Fluoride (NaF)	Millipore Sigma	201154
Dithiothreitol (DTT)	ThermoFisher	R0861
Phenylmethylsulfonyl fluoride (PMSF)	ThermoFisher	36978
cOmplete Protease Inhibitor Cocktail	Millipore Sigma	11697498001
Polyethylenimine, Linear (MW 25,000)	Polysciences, Inc	23966
2-Mercaptoethanol	Millipore Sigma	M3148
Protease Inhibitor Cocktail Set I	Millipore Sigma	539131
Phosphatase Inhibitor Cocktail Set II	Millipore Sigma	524625
Protein A Sepharose CL-4B	GE Healthcare	17078001
Criterion gels	BioRad	5678083
Hoechst 33342	Millipore Sigma	B2261
Sodium tetraborate	Millipore Sigma	221732
Trichostatin A	Millipore Sigma	T8552
Critical Commercial Assays		
DC Protein Assay kit	Bio-Rad	5000111
BCA Protein Assay Kit	ThermoFisher	23225
RNeasy Mini Kit	QIAGEN	74104
FITC BrdU Flow kit	BD Pharmingen	559619
ReliaBLOT IP/Western Blot	Bethyl Laboratories	WB120
Deposited Data		
RNA-Seq	This work	GEO: GSE121857; https://www.ncbi.nlm.nih.gov/gds; GSE121857

REAGENT or RESOURCE	SOURCE	IDENTIFIER
Experimental Models: Cell Lines		
Human: T98G	ATCC	CRL-1690
T98G Sin3B WT (D11)	This work	N/A
T98G Sin3BKO (G6)	This work	N/A
T98G Sin3BKO (B5)	This work	N/A
T98G + EV (pcDNA3.1 + transient transfection)	This work	N/A
T98G + Sin3B-FLAG (pcDNA3.1+ transient transfection)	This work	N/A
T98G Sin3BKO (G6) + EV (pBabe puro – retrovirus)	This work	N/A
T98G Sin3BKO (G6) + Sin3B-FLAG (pBabe puro – retrovirus)	This work	N/A
T98G + Lin9-V5-His (pEF6 – transient transfection)	This work	N/A
T98G + Lin9-V5-His (pEF6 – transient transfection) + Sin3B-FLAG (pcDNA3.1+ transient transfection)	This work	N/A
T98G + shSCRAMBLE (pTRIPZ – lentivirus)	This work	N/A
T98G + shSin3B (pTRIPZ – lentivirus)	This work	N/A
T98G + Cdt1-mKO2 (MaRX hygro – retrovirus) + hGmnn-mAG1 (pLB(N)CX – retrovirus)	This work	N/A
T98G WT (D11) + Cdt1-mKO2 (MaRX hygro – retrovirus) + hGmnn-mAG1 (pLB(N)CX – retrovirus)	This work	N/A
T98G Sin3BKO (G6) + Cdt1-mKO2 (MaRX hygro – retrovirus) + hGmnn-mAG1 (pLB(N)CX – retrovirus)	This work	N/A
T98G Sin3BKO (B5) + Cdt1-mKO2 (MaRX hygro – retrovirus) + hGmnn-mAG1 (pLB(N)CX – retrovirus)	This work	N/A
T98G + Emi1-FLAG (pTRIPZ-Puro – lentivirus)	This work	N/A
T98G WT (D11) + Emi1-FLAG (pTRIPZ-Puro – lentivirus)	This work	N/A
T98G Sin3B (G6) + Emi1-FLAG (pTRIPZ-Puro – lentivirus)	This work	N/A
T98G Sin3BKO (B5) + Emi1-FLAG (pTRIPZ-Puro – lentivirus)	This work	N/A
T98G + Cdt1-mKO2 (MaRX hygro – retrovirus) + hGmnn-mAG1 (pLB(N)CX – retrovirus) + Emi1-FLAG (pTRIPZ-Puro – lentivirus)	This work	N/A
T98G WT (D11) + Cdt1-mKO2 (MaRX hygro – retrovirus) + hGmnn-mAG1 (pLB(N)CX – retrovirus) + Emi1-FLAG (pTRIPZ-Puro – lentivirus)	This work	N/A
T98G Sin3BKO (G6) + Cdt1-mKO2 (MaRX hygro – retrovirus) + hGmnn-mAG1 (pLB(N)CX – retrovirus) + Emi1-FLAG	This work	N/A
T98G Sin3BKO (B5) + Cdt1-mKO2 (MaRX hygro – retrovirus) + hGmnn-mAG1 (pLB(N)CX – retrovirus) + Emi1-FLAG (pTRIPZ-Puro – lentivirus)	This work	N/A
Human: HEK293T	ATCC	CRL-3216
HEK293T + Lin9-V5-His (pEF6 – transient transfection) + EV (pcDNA3.1+ transient transfection)	This work	N/A
HEK293T + Lin9-V5-His (pEF6 – transient transfection) + Sin3B-FLAG (pcDNA3.1 + transient transfection)	This work	N/A
HEK293T + Lin37-V5-His (pEF6 – transient transfection) + EV (pcDNA3.1+ transient transfection)	This work	N/A
HEK293T + Lin37-V5-His (pEF6 – transient transfection) + Sin3B-FLAG (pcDNA3.1 + transient transfection)	This work	N/A
HEK293T + Bmyb-V5 (pcDNA3.1 + transient transfection) + EV (pcDNA3.1+ transient transfection)	This work	N/A
HEK293T + Bmyb-V5 (pcDNA3.1 + transient transfection) + Sin3B-FLAG (pcDNA3.1 + transient transfection)	This work	N/A

REAGENT or RESOURCE	SOURCE	IDENTIFIER
HEK293T + p107-HA (pCMV – transient transfection) + EV (pcDNA3.1+ transient transfection)	This work	N/A
HEK293T + p107-HA (pCMV – transient transfection) + Sin3B-FLAG (pcDNA3.1 + transient transfection)	This work	N/A
HEK293T + p130-HA (pcDNA3.1+ transient transfection) + EV (pcDNA3.1+ transient transfection)	This work	N/A
HEK293T + p130-HA (pcDNA3.1+ transient transfection) + Sin3B-FLAG (pcDNA3.1 + transient transfection)	This work	N/A
HEK293T + Foxm1 (pMyc – transient transfection) + EV (pcDNA3.1+ transient transfection)	This work	N/A
HEK293T + Foxm1 (pMyc – transient transfection) + Sin3B-FLAG (pcDNA3.1 + transient transfection)	This work	N/A
HEK293T + Lin9-V5-His (pEF6 – transient transfection)	This work	N/A
HEK293T + Lin9-V5-His (pEF6 – transient transfection) + Sin3BDHID-FLAG (pcDNA3.1 + transient transfection)	This work	N/A
HEK293T + Lin9-V5-His (pEF6 – transient transfection) + Sin3B (1-304)-FLAG (pcDNA3.1 + transient transfection)	This work	N/A
HEK293T + Lin9-V5-His (pEF6 – transient transfection) + Sin3B (1-510)-FLAG (pcDNA3.1 + transient transfection)	This work	N/A
HEK293T + Lin9-V5-His (pEF6 – transient transfection) + Sin3B (305-1098)-FLAG (pcDNA3.1+ transient transfection)	This work	N/A
HEK293T + Lin9-V5-His (pEF6 – transient transfection) + Sin3B (511-1098)-FLAG (pcDNA3.1+ transient transfection)	This work	N/A
Mouse: Embryonic Fibroblasts (Sin3B KO)	(David et al., 2008)	N/A
MEF Sin3BKO + EV (pBabe puro – retrovirus)	This work	N/A
MEF Sin3BKO + Sin3B-FLAG (pBabe puro – retrovirus)	This work	N/A
Mouse: Embryonic Fibroblasts (Rb KO; p107 KO; p130 KO) (Triple Knock Out, TKO)	(Dannenberg et al., 2000)	N/A
Mouse: NIH 3T3	ATCC	CRL-1658
NIH 3T3 + EV (pcDNA3.1 + transient transfection)	This work	N/A
NIH 3T3 + Sin3B-FLAG (pcDNA3.1+ transient transfection)	This work	N/A
Experimental Models: Organisms/Strains		
Mouse: Sin3B-KO	(David et al., 2008)	N/A
Mouse: TKO (Rb KO; p107 KO; p130 KO) (Triple Knock Out, TKO)	(Dannenberg et al., 2000)	N/A
Oligonucleotides		
pTRIPZ-shSin3B-Puromycin (AGGCTGTAGACATCGTCCA)	Dharmacon	V3THS_315587
Sin3B gRNA #1 FWD: CACCGACCAGGTGAAGATCCGCTT	IDT	N/A
Sin3B gRNA #2 FWD: CACCGAGAAGACGCCCTCACCTATC	IDT	N/A
Sin3B gRNA #3 FWD: CACCGTGCCAAAGCGGATCTTCACC	IDT	N/A
Sin3B gRNA #4 FWD: CACCGATCTCCAGGAAGCCGTTGT	IDT	N/A
Sin3B gRNA #4 FWD: CACCGATCTCCAGGAAGCCGTTGT	IDT	N/A
Sin3B gRNA #5 FWD: CACCGCTCCAGGAAGCCGTTGTAGG	IDT	N/A
Sin3B gRNA #6 FWD: CACCGTCACCTGGTCCAGATAGGTG	IDT	N/A
Recombinant DNA		

REAGENT or RESOURCE	SOURCE	IDENTIFIER
Plasmid: pcDNA3.1 +	ThermoFisher	V79020
Plasmid: pCL-Eco	Addgene	12371
Plasmid: VSV.G	Addgene	14888
Plasmid: Gag/Pol	Addgene	14887
Plasmid: psPAX2	Addgene	12260
Plasmid pMD2.G	Addgene	12259
Plasmid: pBABE-Puro	Addgene	1764
Plasmid: px330-hSpCas9	Addgene	42230
Plasmid: pLB(N)CX	J. DeCaprio (DF/HCC)	N/A
Plasmid: MaRX Ivf Hygromycin	R. DePinho (MD Anderson)	N/A
Plasmid: pFucci-G1 Orange Cloning Vector (Cdt1-mKO2)	MBL	AM-V9001M
Plasmid: pFucci-S/G2/M Green Cloning Vector (hGmnn-hmAGI)	MBL	AM-V9012M
Plasmid: pcDNA3.1-Cdt1-mKO2	This work	N/A
Plasmid: pcDNA3.1-hGmnn-hmAG1	This work	N/A
Plasmid: MaRX Ivf Hygromycin-Cdt1-mKO2	This work	N/A
Plasmid: pLB(N)CX-hGmnn-mAG1	This work	N/A
Plasmid: pTRIPZ-shSCRAMBLE	M. Pagano (NYU)	N/A
Plasmid: pTRIPZ-EMI1-FLAG-Puro	M. Pagano (NYU)	N/A
Plasmid: pcDNA3.1+Sin3B-FLAG	This work	N/A
Plasmid: pcDNA3.1+Sin3BDHID-FLAG	This work	N/A
Plasmid: pcDNA3.1+Sin3B (1–304)-FLAG	This work	N/A
Plasmid: pcDNA3.1+Sin3B (1–510)-FLAG	This work	N/A
Plasmid: pcDNA3.1+Sin3B (305–1098)-FLAG	This work	N/A
Plasmid: pcDNA3.1+Sin3B (511–1098)-FLAG	This work	N/A
Plasmid: pBabe-Lin37-V5-Hygro	(Litovchick et al., 2007)	N/A
Plasmid: pEF6-Lin9-V5-His	(Litovchick et al., 2007)	N/A
Plasmid: pEF6-Lin37-V5-His	(Litovchick et al., 2007)	N/A
Plasmid: pcDNA3.1+ Bmyb-V5	(Litovchick et al., 2007)	N/A
Plasmid: pCMV-p107-HA	(Litovchick et al., 2007)	N/A
Plasmid: pcDNA3.1+p130-HA	(Litovchick et al., 2007)	N/A
Plasmid: Myc-FoxM1	P. Raychaudhuri (UIC)	N/A
Software and Algorithms		
CRISPR Design	Feng Zhang	http://crispr.mit.edu/
FastQC	Simon Andrews	https://www.bioinformatics.babrahamac.uk/projects/fastqc/
Trimmomatic	(Bolger et al., 2014)	http://www.usadellab.org/cms/?page=trimmomatic
TopHat	(Trapnell et al., 2009)	https://ccb.jhu.edu/software/tophat/index.shtml
HTSeq-count	(Anders et al., 2015)	https://htseq.readthedocs.io/en/release_0.10.0/
edgeR	(Robinson et al., 2010)	https://bioconductor.org/packages/release/bioc/html/edgeR.html
GSEA	(Subramanian et al., 2005)	http://software.broadinstitute.org/gsea/index.jsp
Enrichr	(Chenetal., 2013)	http://amp.pharm.mssm.edu/Enrichr/

REAGENT or RESOURCE	SOURCE	IDENTIFIER
Sequest	(Eng et al., 1994)	http://fields.scripps.edu/yates/wp/?page_id=17
Prism	GraphPad Software	https://www.graphpad.com/scientific-software/prism/
FloJo	FloJo, LLC	https://www.fiowio.com/